# Analysis of bifurcation patterns in reaction-diffusion systems: Effect of external noise on the Brusselator model

Srinivas S. Yerrapragada,* Jayanta K. Bandyopadhyay,† V. K. Jayaraman,‡ and B. D. Kulkarni‡
*Chemical Engineering Department, University of Louisville, Louisville, Kentucky 40292*
(Received 31 July 1996; revised manuscript received 10 December 1996)

A detailed stochastic analysis of the Brusselator scheme has been performed to bring out the effect of external noise on the system. The diffusion parameter $D_x$ was taken to be fluctuated by external noise and a complete solution diagram with the composition variables $X$ and $Y$ has been generated. These noise-induced transitions reveal that this system attains a stable state not described by its deterministic analysis. The stochastic analyses also reveal that the structural stability of such systems is disturbed even for a slight external perturbation in the bifurcation parameter, and in a certain range of noise intensity ($\sigma$) and correlation time ($\tau$) some different spatial and temporal structures arise. [S1063-651X(97)08505-X]

PACS number(s): 05.45.+b

## INTRODUCTION

One of the most striking and intriguing aspects of natural phenomena is that complex systems, involving a large number of strongly interacting elements, can form and maintain ''patterns of order'' extending over a macroscopic space and time scale. Oscillatory as well as multiple steady-state behavior of certain catalytic reactions has been observed in numerous experiments and a number of theoretical investigations have been attempted to explain these effects [1]. Sustained oscillations in reaction rate, in the concentration of a reacting component, or in the temperature have been noticed in many heterogeneous catalytic systems. It has been established that for the nonisothermal systems it is usually the thermal feedback that causes oscillations, while for the isothermal operations it is generally the autocatalytic variable. Particular attention has been paid in the literature to the isothermal oscillations of hydrogen or carbon monoxide on catalytic wires, gauzes, or supported catalysts. In many situations the oscillations have been aperiodic or irregular. Very complex oscillations in the case of isothermal oxidation of carbon monoxide over a single porous catalyst particle have been reported [2]. It is generally recognized that the physical processes of heat and mass transfer, coupled with nonlinear kinetics may be responsible for the periodic phenomena. It has been observed, however, that the majority of the proposed models predict simple oscillations, or the relaxation type of oscillations, but no model adequately accounts for multipeak or chaotic oscillations.

Among the few models that explain the aperiodic oscillations are the ''pebbly bed'' model (a metal catalyst finely disperged on an inactive carrier) [3,4], and the coverage-dependent activation energy model [5]. The essence of all these proposed models is the presence of a discrete number of oscillators (metal crystallites or surface patches), which if weakly connected can lead to chaotic oscillations due to desynchronization [6].

It is widely known that the interaction of a reaction and diffusion in an open system operating far from equilibrium gives rise to many interesting phenomena such as ordered steady states, spatially homogeneous periodic solutions, traveling waves and fronts, and shock structures. The volume of literature in this field has been growing steadily since the classical paper by Nicolis and Prigogine [7]. The reaction-diffusion equations coupled with appropriate kinetic expressions have been shown to serve as simple models of a number of biological phenomena and may also explain similar phenomena in many other fields.

A simple model known as the Brusselator [8] shows how structure can arise as a sequence of instabilities. Evidently, under certain circumstances the usual equilibrium state of a chemical reaction may be unstable with respect to small perturbations and a spatially nonuniform steady state appears (symmetry-breaking instability). For the Brusselator chemical network, a couple of results of the numerical solution of the transient reaction-diffusion equation were reported [9]. They have calculated multiple stable solutions for particular values of governing parameters. A slight change of initial conditions for the relevant parabolic equations very often resulted in widely different steady-state profiles. As a result, it was not possible to determine how many solutions exist for given values of the parameters. Kubicek and Marek [10] took advantage of the continuous approach that made it possible to draw a complete bifurcation diagram. Almost all authors considered the initial components $A$ and $B$ to somehow be maintained uniformly so that they can be treated as externally determined parameters. An exception is the work of Herschkowitz-Kaufman [9], which indicated that if diffusion of $A$ is considered, the space structures still may exist. A detailed study of this scheme has been made and reported for all the possible situations [11]. This work was further extended to show the chaotic behavior of this system through period-doubling bifurcation [12].

It is well known that nonlinear macroscopic systems operating far from equilibrium possess points of branching (bifurcation points) at which the stability properties of the steady-state solutions undergo change. At these so-called

*Present address: Simulation & Advanced Controls, Inc., Louisville, KY 40202.
†Present address: United Catalyst Inc., Louisville, KY 40232.
‡National Chemical Laboratory, Pune 411 008, India.

 

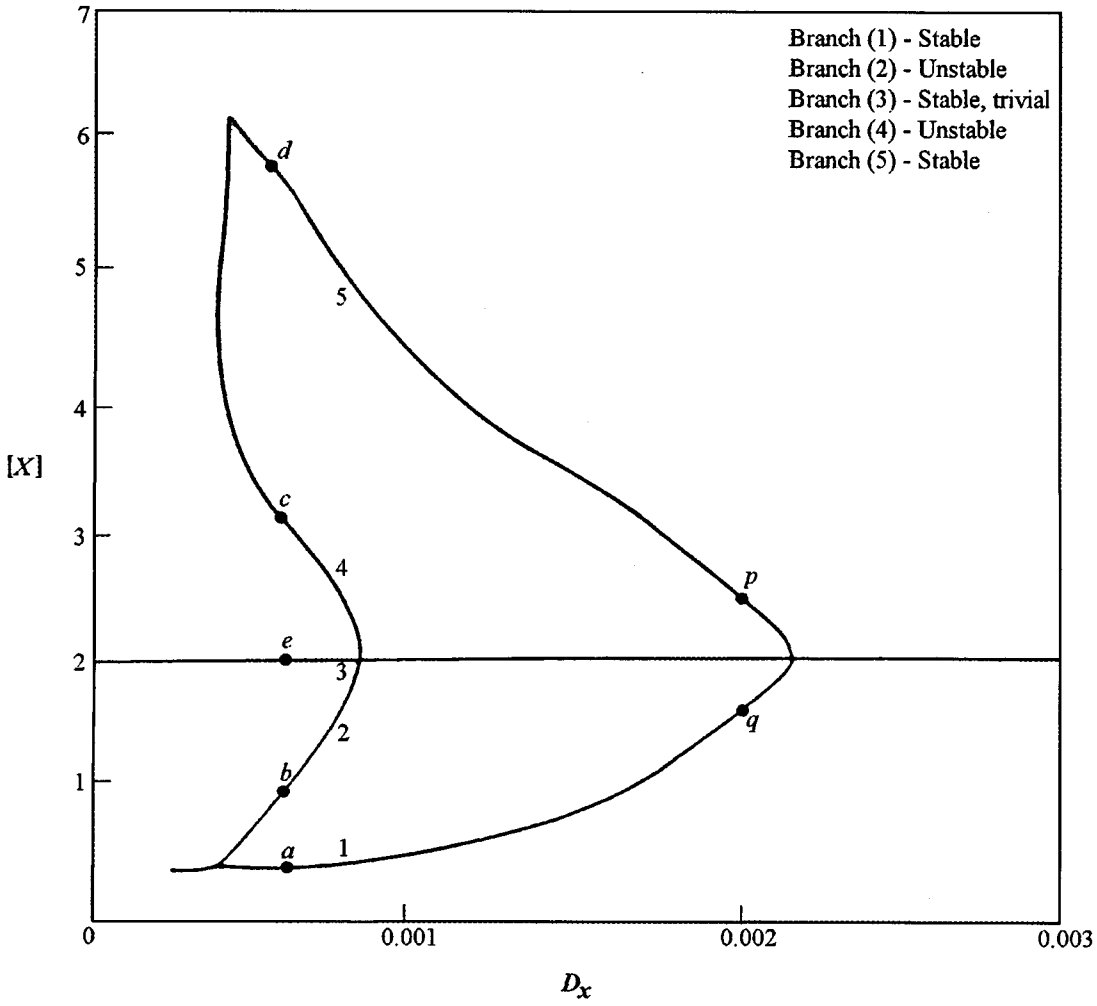


FIG. 1. Bifurcation diagram showing the dependence of the concentration variable $X$ on the diffusion component $D_x$ for $L=0.1$, $D_y=0.008$, $A=2$, and $B=4.6$.

transition points the behavior of the macroscopic systems is extremely sensitive to perturbations and the mechanisms that ensure the regression or decay of these fluctuations are generally lacking. It is necessary then to explicitly take account of these fluctuations in modeling systems operating under such conditions, by the use of stochastic methods. The perturbations are inherent in most systems and are referred to as the internal or external noise depending on whether the origin of these perturbations lie within the system or outside it, such as the environment. The role of internal noise in modifying the behavior of macroscopic systems has been extensively investigated using the master equation formalism or by a continuous diffusion process, i.e., the Fokker-Planck equation [13,14]. It is now agreed that the contribution of internal noise to the macroscopic evolution equations is generally proportional to the inverse of the square-root volume of the system. This implies that for large-volume globally stable systems this effect can generally be ignored. However, for systems in the neighborhood of instability the inclusion of noise leads to large deviations and qualitatively different results from those obtained for the macroscopic systems. Besides this internal noise, the origin of the perturbations in the system may also lie external to the system. This can occur, for example, when the system is coupled to a fluctuating environment. These fluctuations may be represented as noise terms in the evolution equation and are referred to as external noise. It may be noticed that these fluctuations occur at a macroscopic level and can be included in the macroscopic description once their statistical properties are known. The incorporation of external noise in the macroscopic equations generates the stochastic differential equation, which can be equivalently written as the Fokker-Planck equations. As would be evident, these fluctuations being external have no bearing on properties of systems such as size or volume. These can therefore be important for large-volume globally stable systems.

The macroscopic equation suitably appended to include the contributions from the external noise takes the form

$$\frac{dx}{dt}=F(x)+G(x)\xi(t) \tag{1}$$

where $x$ is the global macroscopic variable (generally an $n$-dimensional vector), $F(x)$ and $G(x)$ are some $n$-dimensional vectorial nonlinear functions of variable $x$, and $\xi(t)$ refers to the stochastic variable with vanishing

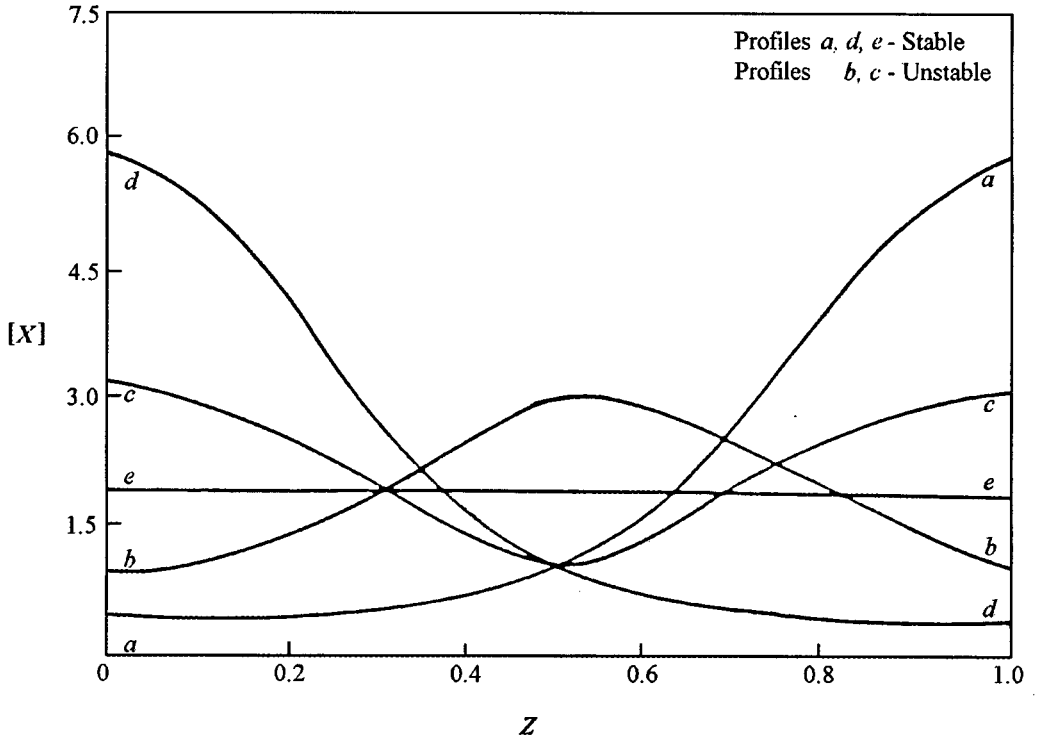


FIG. 2. Steady-state profiles of the concentration variable $X$ for $L=0.1$ and $D_x=0.0006$.

mean value. The function $F(x)$ characterizes the deterministic part of the evolution of the system and $G(x)$ describes the coupling of the variable $x$ to the external noise $\xi(t)$. This coupling is termed additive if $G(x)$ is constant (independent of $x$) and is termed multiplicative if $G(x)$ is dependent on $x$. These two type of couplings have different properties: while the additive noise would not influence the stability properties of the macroscopic equation (because eigenvalues of the Jacobian matrix are not affected), the multiplicative noise may bring about changes in the stability properties of the system, sometimes even to a completely new evolution pattern. The multiplicative noise can enter either as a linear, a quadratic, or an exponential form or as a dichotomic noise. In this work only the linear coupling of the multiplicative noise is considered.

It is an experimental observation that in most situations the magnitudes of external fluctuations are distributed according to a curve that is satisfactorily described by the bell-shaped curve of the Gaussian or the normal distribution. This fact can be understood as a consequence of a fundamental theorem of probability theory, known as the central limit theorem. One can utilize the fact that, in most situations, fluctuations in external parameters (such as flow rate, temperature, and pressure) cannot be attributed to any one particular cause and are the result of the cumulative effect of numerous environmental or instrumental factors. If these factors are not too dissimilar and are not strongly correlated, the central limit theorem ensures that a Gaussian distribution would result in the external fluctuating parameter. It is usually assumed that $\xi(t)$ represents a Gaussian process with zero mean and is $\delta$ correlated [15–17].

In this paper a detailed stochastic analysis of the Brusselator scheme for one particular characteristic length has been done. A complete solution diagram of the diffusion parameter $D_x$ with the composition variables $X$ and $Y$ has been generated and the diffusion parameter was taken to be fluctuated by external source. The results thus obtained reveal that the structural stability of the deterministic states can get disturbed even for slight external perturbations and in some cases new structures arise.

## THE BRUSSELATOR MODEL

The reaction sequence taking place for a typical Brusselator under open system conditions can be obtained as

$$A \underset{}{\overset{k_1}{\rightleftarrows}} B, \tag{2a}$$

$$B + X \overset{k_2}{\rightleftarrows} Y + D, \tag{2b}$$

$$2X + Y \overset{k_3}{\rightleftarrows} 3X, \tag{2c}$$

$$X \overset{k_4}{\rightleftarrows} E. \tag{2d}$$

Such reactions as represented by the above scheme can be visualized as enzymatic (catalyzed by enzymes immobilized on solid support) that take place inside the ''idealized pores'' (pores of uniform radii but different lengths) of a catalyst pellet. It can be assumed that these idealized pores have blocked ends and hence act as oscillators under certain conditions. This model has been mainly chosen for its autocatalytic properties and limit cycle behavior. The analysis of the problem is simplified by assuming that the noncatalytic com-

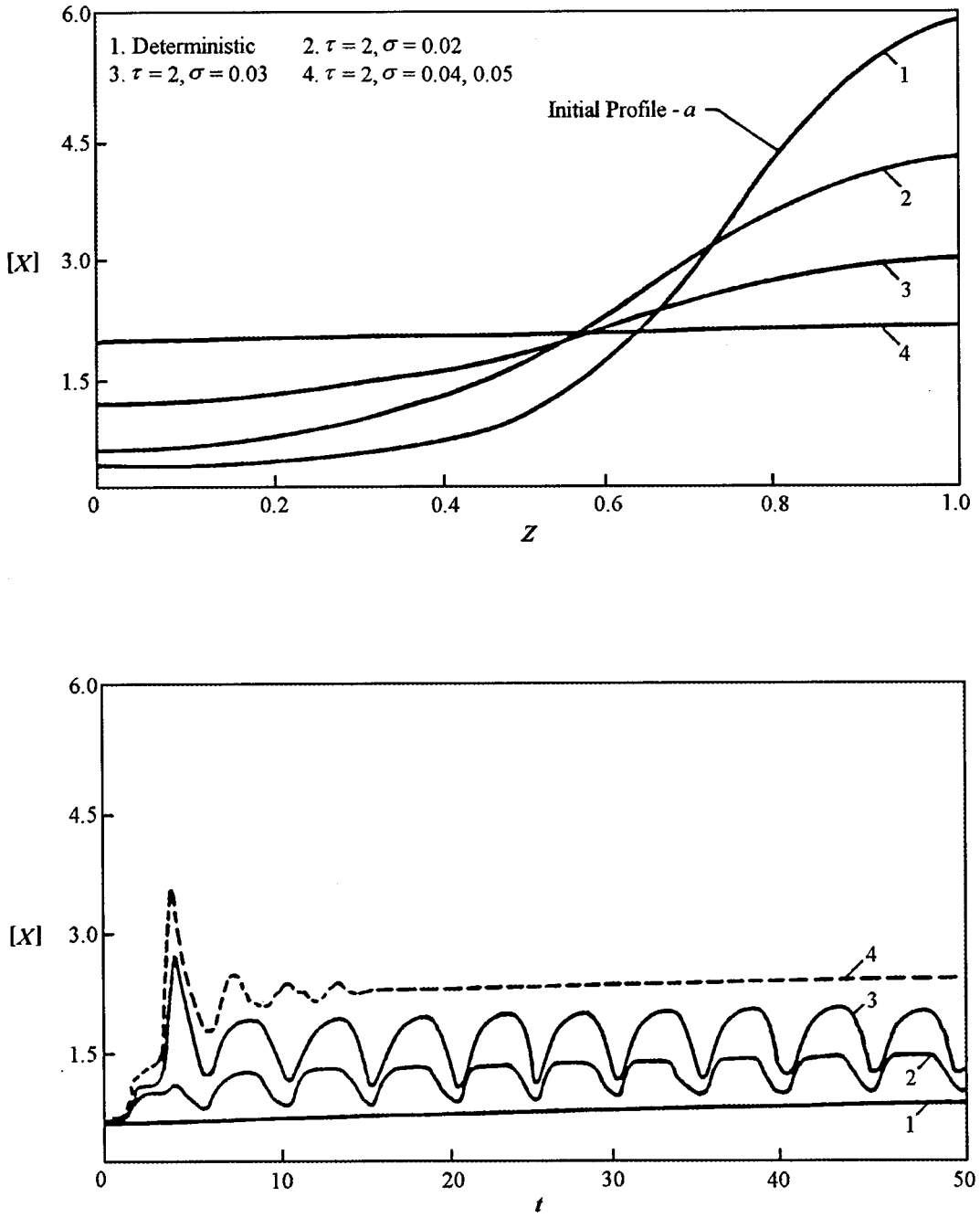


FIG. 3. Spatial and temporal profiles of the concentration variable $X$ for a fixed value of the noise correlation time and varying noise intensity for $L=0.1$, $D_x=0.0006$, and initial profile $a$.

ponents $A$ and $B$ have very high diffusion coefficients as compared to the autocatalytic components $X$ and $Y$ and can therefore be regarded as constant in the reaction. The net reaction for the above scheme is

$$A+B\rightarrow D+E. \tag{3}$$

The corresponding balance equations can be written as

$$\frac{d\overline{X}}{dt}=k_1\overline{A}-(k_2\overline{B}+k_4)\overline{X}+k_3\overline{X^2Y}, \tag{4}$$

$$\frac{d\overline{Y}}{dt}=k_2\overline{BX}-k_3\overline{X^2Y}, \tag{5}$$

where the overbars over the variables denote that they are the actual prescaled reaction components. Now, by introducing the scaled variables

$$t=k_4\overline{t}, \quad X=\left(\frac{k_3}{k_4}\right)^{1/2}\overline{X}, \quad Y=\left(\frac{k_3}{k_4}\right)^{1/2}\overline{Y}; \tag{6}$$

$$A=\left(\frac{k_1^2k_3}{k_4^3}\right)^{1/2}\overline{A}, \quad B=\left(\frac{k_2}{k_4}\right)\overline{B}, \tag{7}$$

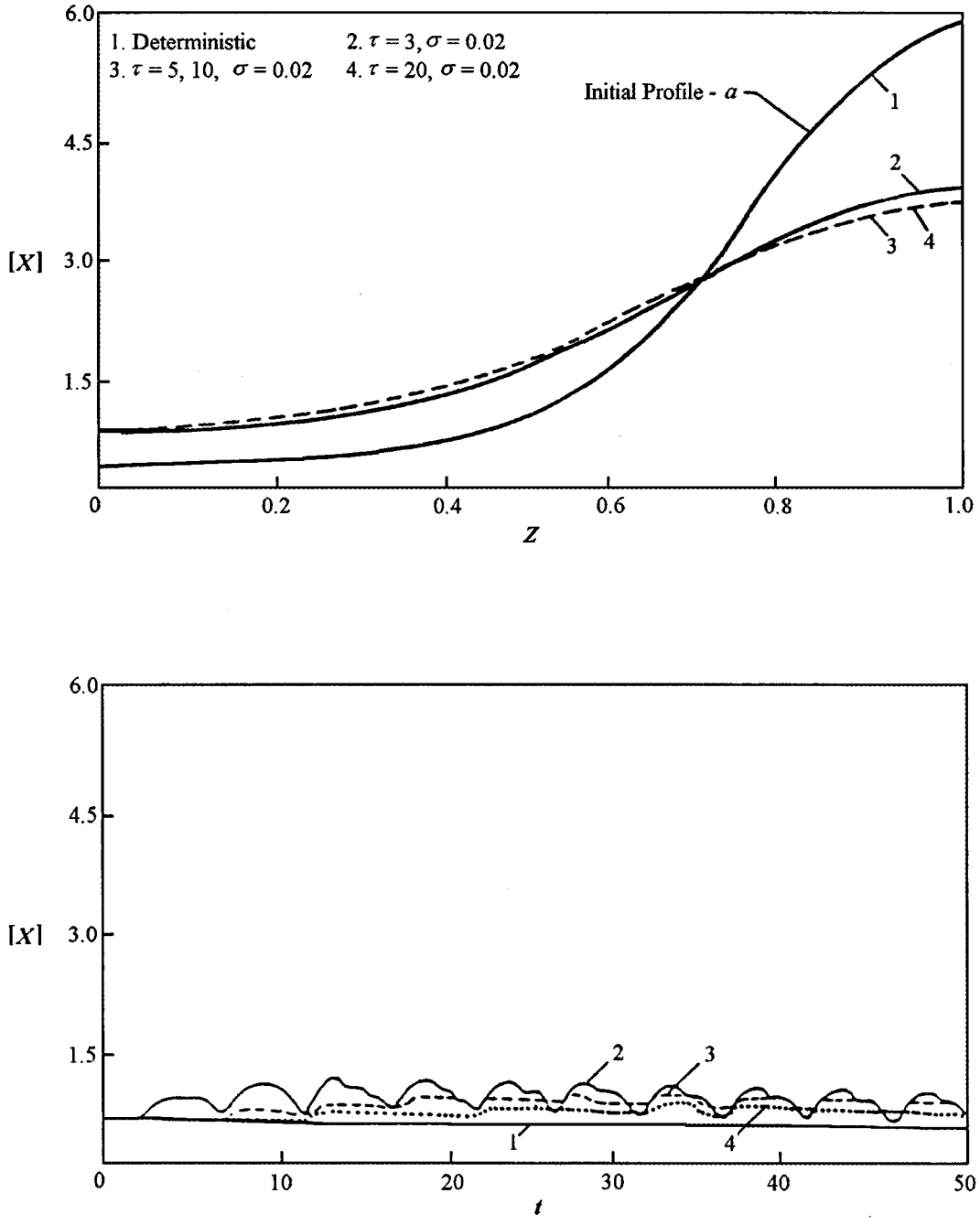


FIG. 4. Spatial and temporal profiles of the concentration variable $X$ for a fixed value of noise intensity and varying noise correlation time for $L=0.1$, $D_x=0.0006$, and initial profile $a$.

we have

$$f(X,Y)=A-(B+1)X+X^2Y, \tag{8}$$

$$g(X,Y)=BX-X^2Y. \tag{9}$$

Considering now a reaction-diffusion system with one-dimensional diffusion components $D_x$ and $D_y$, the balance equations can be represented by the two parabolic partial differential equations

$$\frac{\partial X}{\partial t}=\frac{D_x}{L^2}\frac{\partial^2 X}{\partial z^2}+f(X,Y), \tag{10}$$

$$\frac{\partial Y}{\partial t}=\frac{D_y}{L^2}\frac{\partial^2 Y}{\partial z^2}+g(X,Y), \tag{11}$$

where $L$ is the characteristic length of the system. The initial condition and the associated boundary conditions of the zero-flux type are given as follows: for the initial conditions

$$t=0, \quad X=X_0, \quad Y=Y_0; \tag{12a}$$

for $z=0$,

$$\frac{dX}{dz}=0=\frac{dY}{dz}; \tag{12b}$$

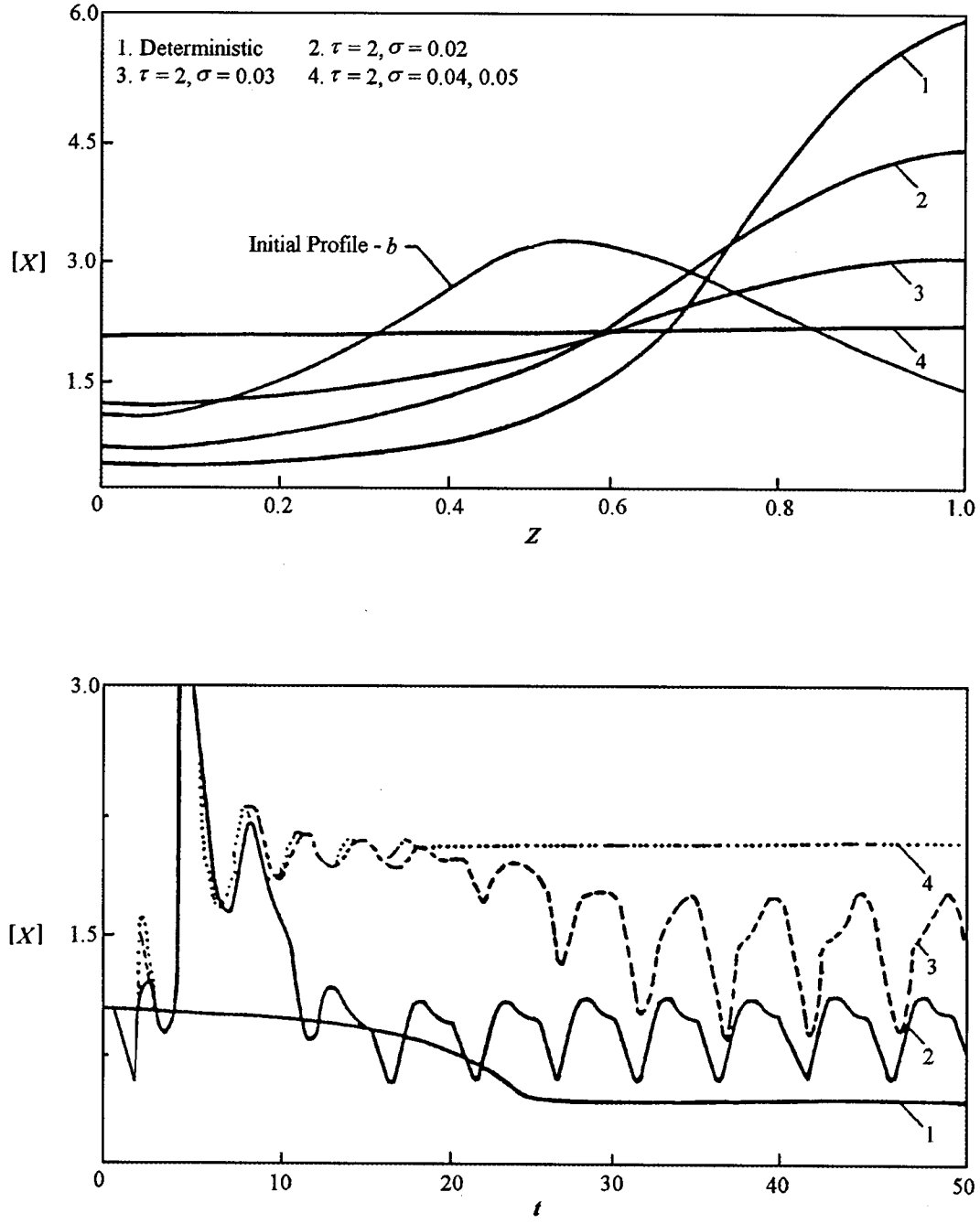


FIG. 5. Spatial and temporal profiles of the concentration variable $X$ for a fixed value of the noise correlation time and varying noise intensity for $L=0.1$, $D_x=0.0006$, and initial profile $b$.

and for $z=1$,

$$\frac{dX}{dz}=0=\frac{dY}{dz}. \tag{12c}$$

## FORMULATION OF THE STOCHASTIC MODEL

For noise with nonvanishing correlation time, the temporal evolution of the system is no longer Markovian. Thus the well-known tools of the Markov processes cannot be applied and it becomes difficult to obtain exact explicit results. However, Horsthemke and Lefever have presented a detailed discussion on the validity of assuming the environment to have certain Markovian properties and the importance of such an approximation [15]. It is also assumed that the environment besides being Markovian is ergodic. Thus the environment is governed by an Ornstein-Uhlenbeck process and hence the external fluctuations can be characterized by the correlation function

$$\frac{d\xi}{dt}=-\frac{1}{\tau}\,\xi+\frac{\sigma}{\sqrt{\tau}}\left(\frac{dW}{dt}\right), \tag{13}$$

where $\xi$ is the noise term, $\sigma$ is the strength of the noise, and

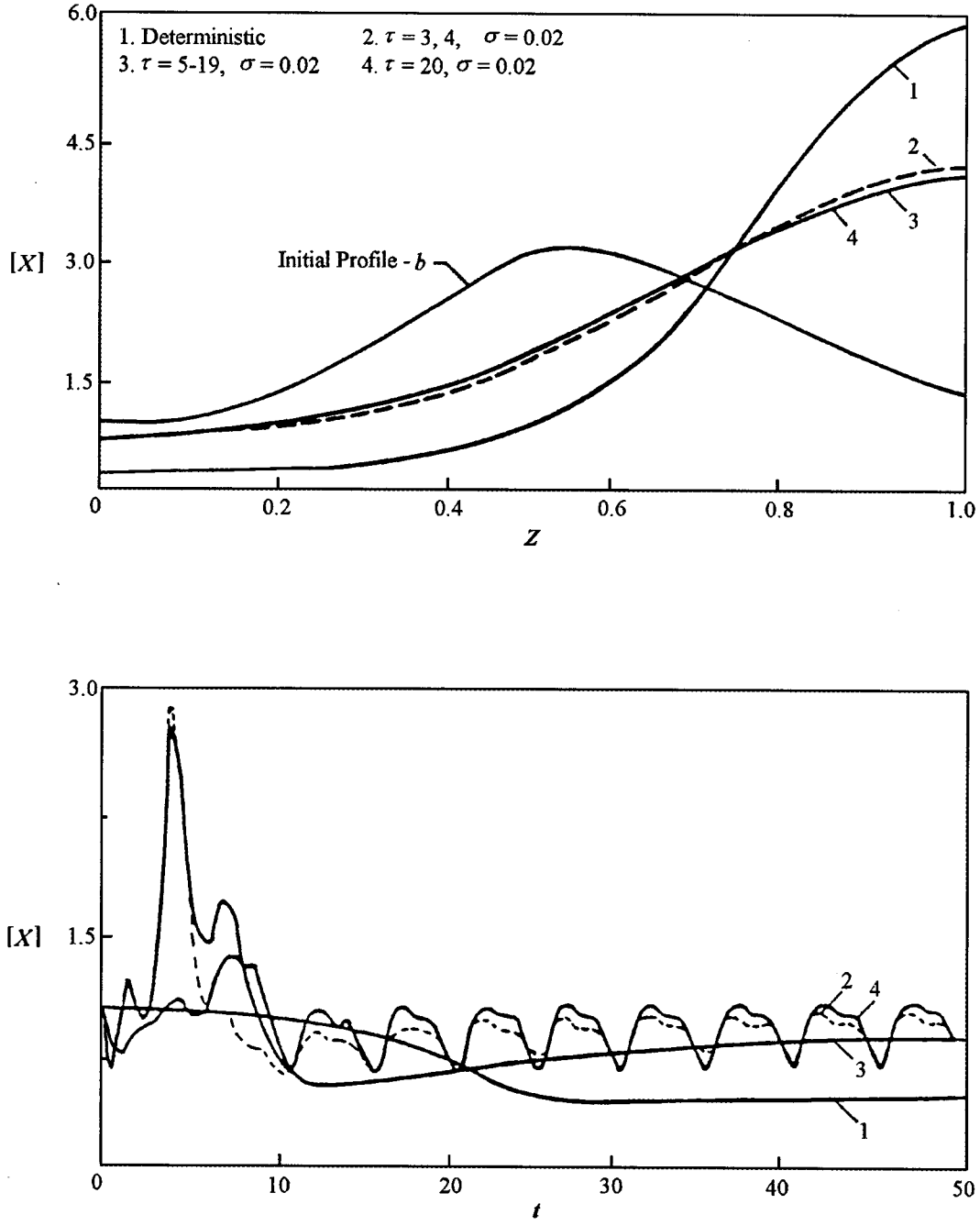


FIG. 6. Spatial and temporal profiles of the concentration variable $X$ for a fixed value of the noise intensity and varying noise correlation time for $L=0.1$, $D_x=0.0006$, and initial profile $b$.

$\tau$ is the correlation time of the noise. $W$ represents the Wiener process, the derivative of which is essentially a pseudo random variable that is characterized by a Gaussian distribution. The noise term $\xi$ has a nonvanishing correlation time and hence is termed as colored noise. The incorporation of this correlation time $\tau$ into the temporal evolution of the system is accomplished by a perturbation expansion method [15]. In the present work $D_x$ is considered to be the fluctuating parameter and is linearly coupled to the external noise in a multiplicative fashion. It should be noted here that the external noise would also affect $D_y$ in some fashion. However, for the sake of simplicity $D_x$ alone is considered to be fluctuating. This assumption is made with a view that because of the coupled nature of the reaction scheme, the structures that emerge due to the fluctuations in $D_x$ should reveal the qualitative behavior of the system in the presence of external disturbances. The effect of these fluctuations takes the form of $\xi/\sqrt{\tau}$ in the spatial direction and can be incorporated into the balance equations in a multiplicative fashion as

$$\frac{\partial X}{\partial t} = A-(B+1)X+X^2Y+\frac{D_x}{L^2}\frac{\partial^2 X}{\partial z^2}+\frac{1}{L^2\sqrt{\tau}}\,\xi(t)\,\frac{\partial^2 X}{\partial z^2}, \tag{14}$$

$$\frac{\partial Y}{\partial t} = BX-X^2Y+\frac{D_y}{L^2}\frac{\partial^2 Y}{\partial z^2}. \tag{15}$$

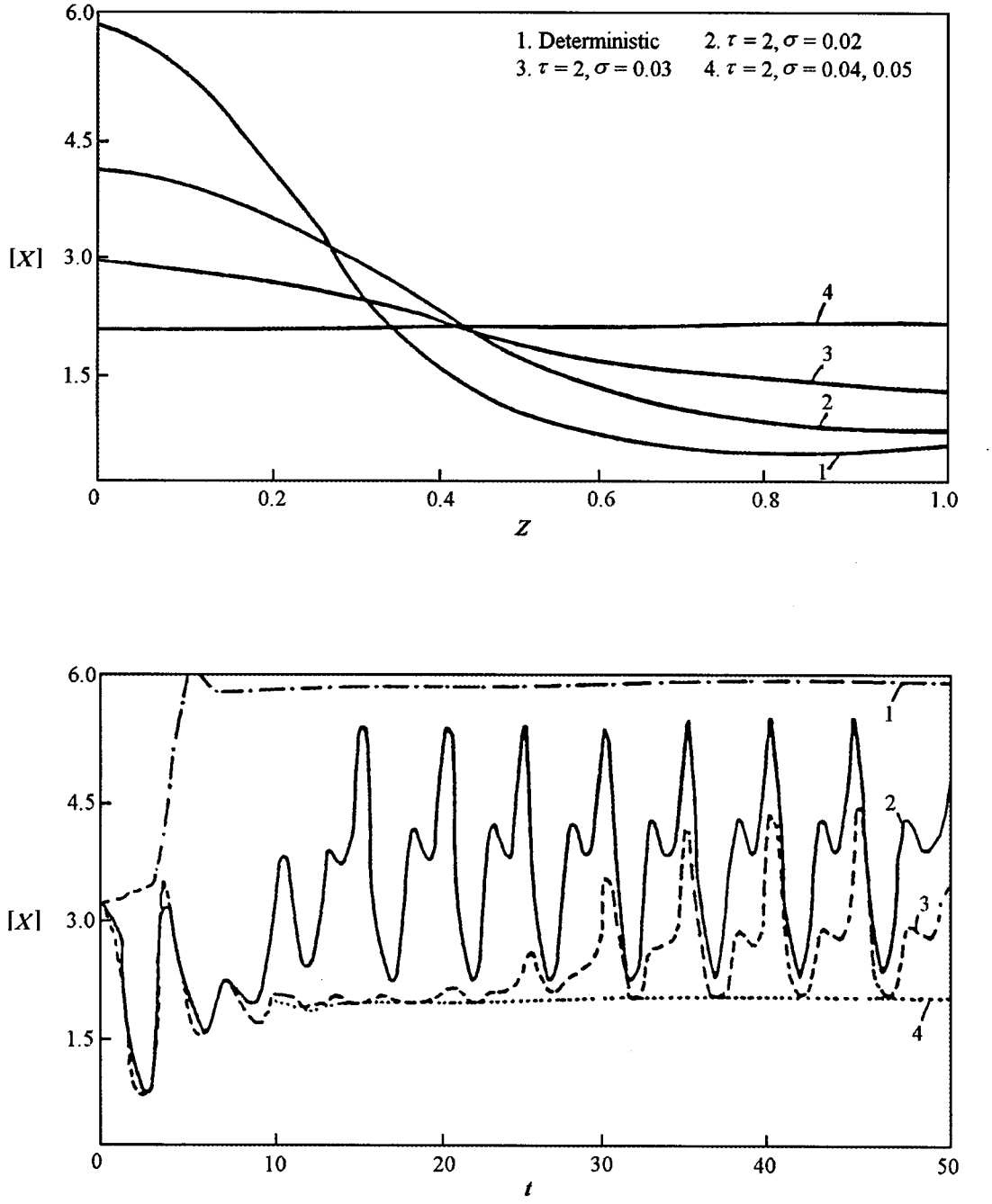


FIG. 7. Spatial and temporal profiles of the concentration variable $X$ for a fixed value of the noise correlation time and varying noise intensity for $L=0.1$, $D_x=0.0006$, and initial profile $c$.

Now the stochastic system dynamics will be described by Eqs. (13)–(15) with the initial and boundary conditions given by Eq. (12).

## NUMERICAL METHODS OF SOLUTION

The two bounded equations [Eqs. (10) and (11)] at steady state reduce to a set of second-order differential equations. The entire bifurcation diagram, which shows the concentration ($X$) dependence on the diffusion parameter ($D_x$), was then constructed by solving these steady-state deterministic equations using the general parametric mapping (GPM) technique [18]. This technique takes advantage of the implicit function theorem and the shooting method as well. For the entire specified operating range of the parameter ($D_x$), the GPM routine solves the system of bounded differential equations for the solution diagram (concentration variable $X$). The steady-state spatial profiles of this set of equations are generated using the Newton-Fox shoot method [19]. In the shooting method, the boundary value problem is transformed into an initial-value problem and the integration of the resulting initial-value problem is carried out by a fourth-order Runge-Kutta method. A guess is made initially for the values of the concentration variables at one end of the space dimension and a forward integration is carried out until the bound

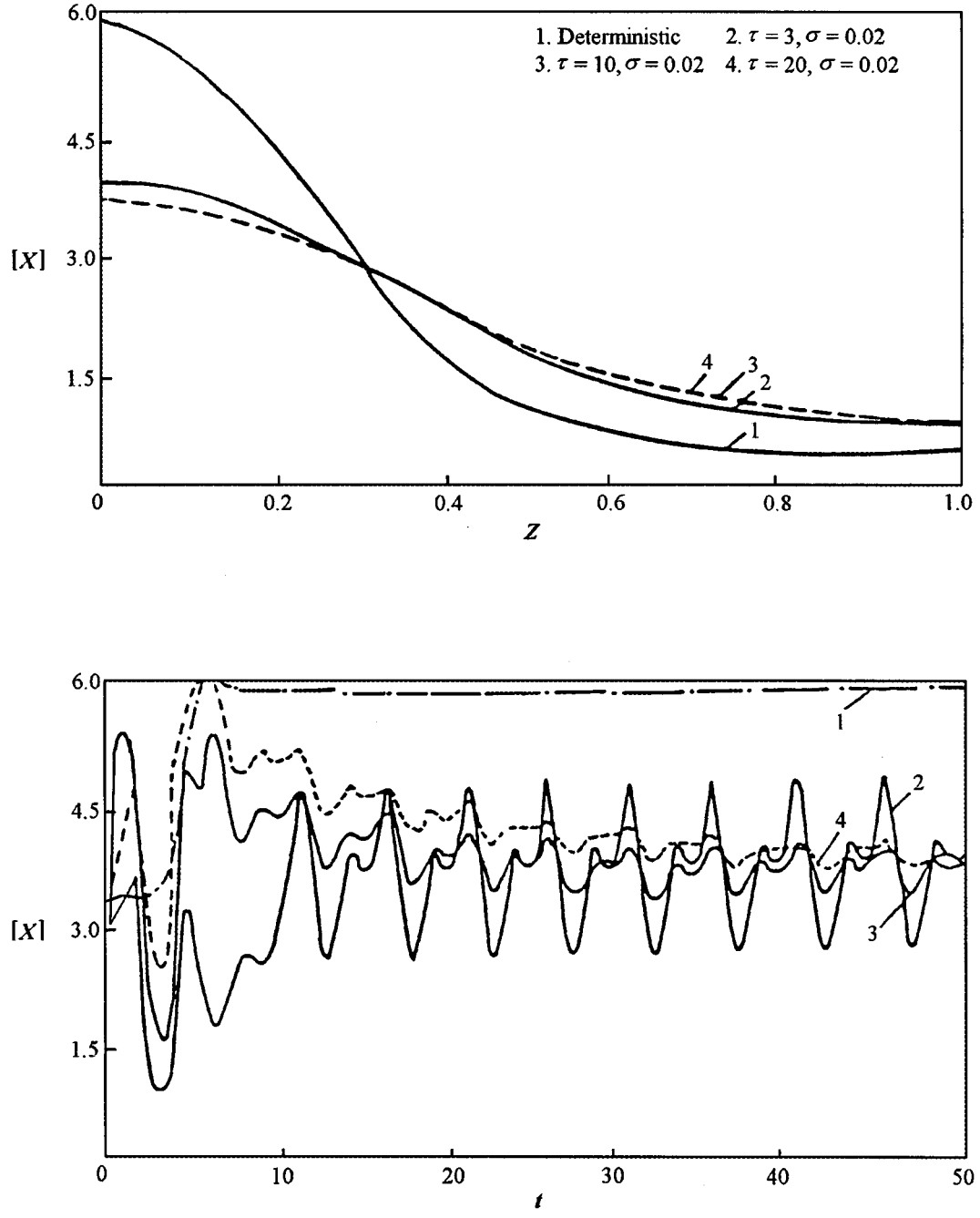


FIG. 8. Spatial and temporal profiles of the concentration variable $X$ for a fixed value of the noise intensity and varying noise correlation time for $L=0.1$, $D_x=0.0006$, and initial profile $c$.

ary conditions at the other end are matched. The temporal evolution of both the deterministic and the stochastic partial differential balance equations [Eqs. (10) and (11) and Eqs. (14) and (15)] along with their boundary conditions [Eq. (12)] is computed using a finite-difference method [20]. This algorithm employs an implicit method, called the Crank-Nicholson method, for reasons of numerical stability. These noise incorporated partial differential equations [Eqs. (14) and (15)] are solved simultaneously with the ordinary differential characteristic noise equation [Eq. (13)], where a pseudo-random-number generator of the Gaussian distribution is used to generate the noise term $\xi$.

## RESULTS AND DISCUSSION

Figure 1 shows a bifurcation diagram with $D_x$ as a parameter and with fixed values of $L$, $D_y$, $A$, and $B$. The trivial solution can be obtained as $X=A$ and $Y=B/A$. The points $a$, $b$, $c$, $d$, and $e$ are chosen in the five-steady-state region of the branches 1, 2, 4, 5, and 3, respectively. The corresponding value of $D_x$ exhibiting these five steady states is 0.0006. From the deterministic analysis the stability of the steady-state profiles has been judged as follows: profiles $a$, $d$, and $e$ are stable and profiles $b$ and $c$ are unstable.

The steady-state profiles for the points $a$, $b$, $c$, $d$, and $e$

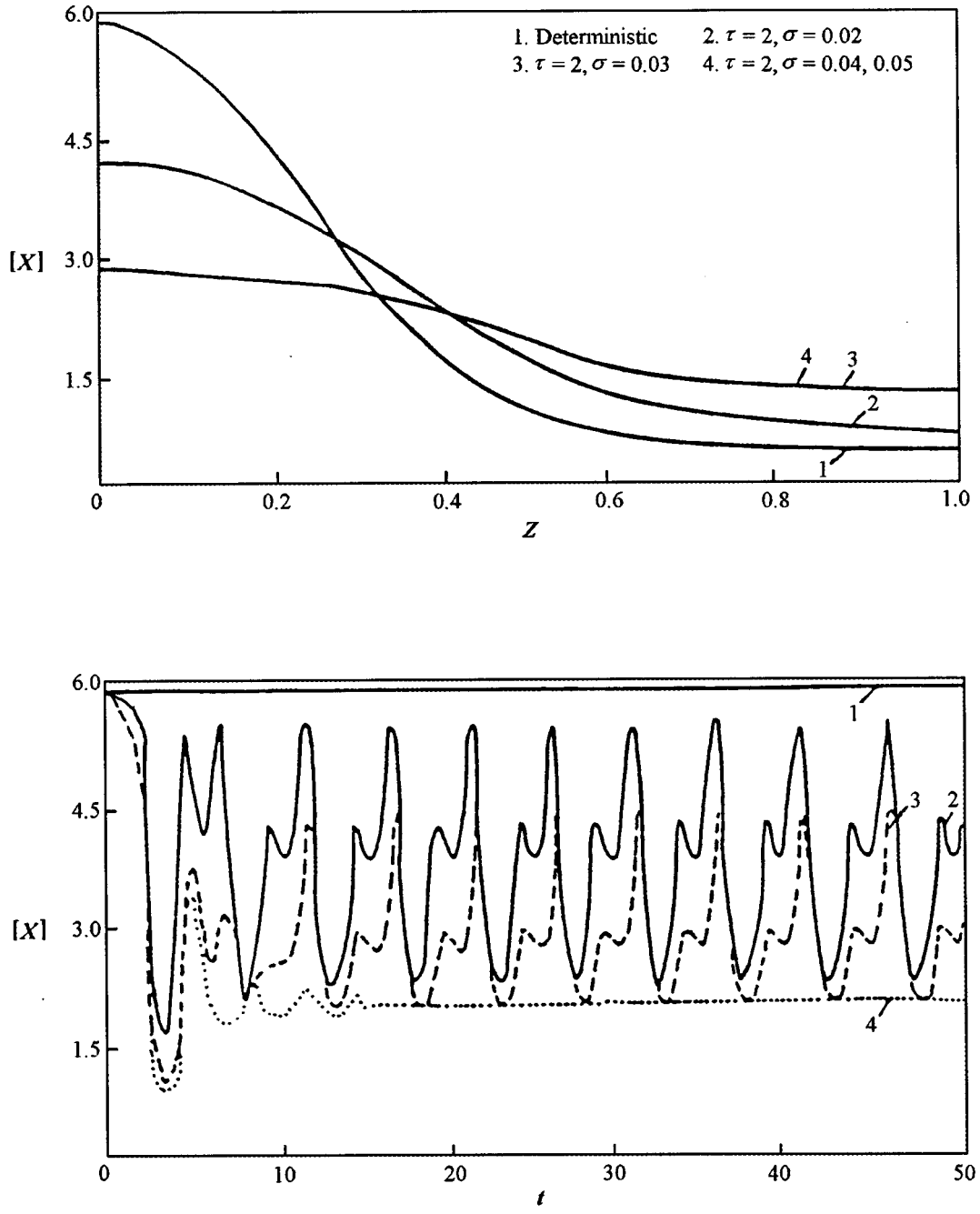


FIG. 9. Spatial and temporal profiles of the concentration variable $X$ for a fixed value of the noise correlation time and varying noise intensity for $L=0.1$, $D_x=0.0006$, and initial profile $d$.

are given in Fig. 2. The profiles indicate how the steady states emerge in the space dimension for the dimensionless concentration variable $X$. The point $a$ shown in Fig. 1 indicates the concentrations of $X$ at the inlet of the characteristic length (i.e., at $z=0$). The other end, i.e., $z=1$, in Fig. 2 corresponds to the characteristic length $L=0.1$. In this study of the Brusselator scheme, the plots are given only for one concentration variable ($X$) and the qualitative features are described on these figures. For the inlet values of the concentration variables $X$ and $Y$, a guess was made at the other end ($z=1$) and a forward integration was performed until the boundary conditions at $z=0$ were matched. These steady-state profiles have been subsequently taken as initial profiles for both deterministic and stochastic analyses.

The effects of $\sigma$ (strength of the noise) and $\tau$ (noise correlation time) on the spatial as well as time evolution of the concentration variable $X$ are given in Figs. 3 and 4. The initial concentration profile $a$ (of Fig. 2) is also marked as 1. The temporal evolution of this profile shows that deterministically (in the absence of noise) it is a stable steady state. These temporal profiles are drawn at the entry conditions ($z=0$). The same initial profile $a$ has been subjected to external fluctuations for varying noise intensity ($\sigma = 0.02-0.05$) at a fixed noise correlation time ($\tau=2$). Now, with the noise incorporated, the spatial profiles in Fig. 3 reveal that for $\sigma=0.02$ the steady state stabilizes at a profile

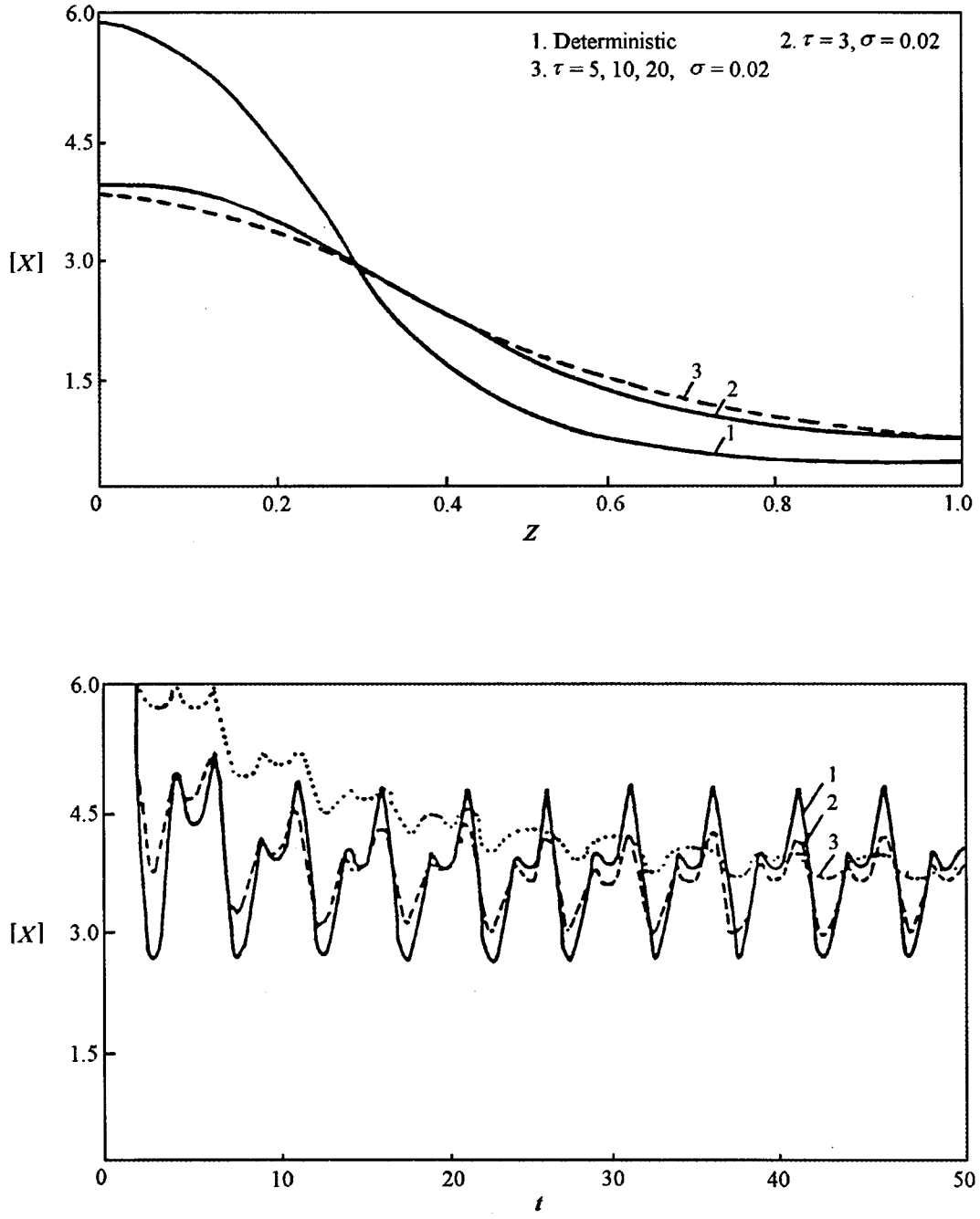


FIG. 10. Spatial and temporal profiles of the concentration variable $X$ for a fixed value of the noise intensity and varying noise correlation time for $L=0.1$, $D_x=0.0006$, and initial profile $d$.

marked 2, for $\sigma=0.03$ stabilizes at a profile marked 3, and for $\sigma=0.02,0.05$ stabilizes at the profile marked 4, for a fixed value of $\tau=2$. It clearly shows that the spatial profiles of $a$ go through new transient profiles for noise strengths of $\sigma=0.02,0.03$, and for higher values of $\sigma=0.04,0.05$ the profiles stabilize at the trivial solution (curve $e$ in Fig. 2).

Figure 4 reveals the results of the effect of $\tau$ on the initial profile $a$. As observed earlier in the effect of $\sigma$, the effect of $\tau$ also brings about new transient profiles for noise correlation times of $\tau=3-20$, for a fixed $\sigma=0.02$. For $\tau<5$ the system stabilizes to the profile marked 2, whereas for $\tau=5-20$ the system stabilizes to the profiles marked 3 and 4. The interesting feature to be observed in this is that unlike the effect of $\sigma$, which takes the solution $a$ to a trivial solution, the effect of $\tau$ brings in a completely new solution during the spatial evolution. The temporal evolution of $X$ reveals the same effect as that of $\sigma$, i.e., periodic oscillations exist for lower values of $\tau$ and with the increase in $\tau$ they become aperiodic as they approach the new steady state. The central phase plane plot of the concentration variables $X$ and $Y$ at $z=0.5$ for $\sigma=0.02$ and $\tau=2$ is depicted in Fig. 11.

Figure 5 gives the deterministic as well as the stochastic solutions (effect of $\sigma$) of the unstable steady-state solution $b$ (see Fig. 2). The initial profile $b$ has been redrawn here to

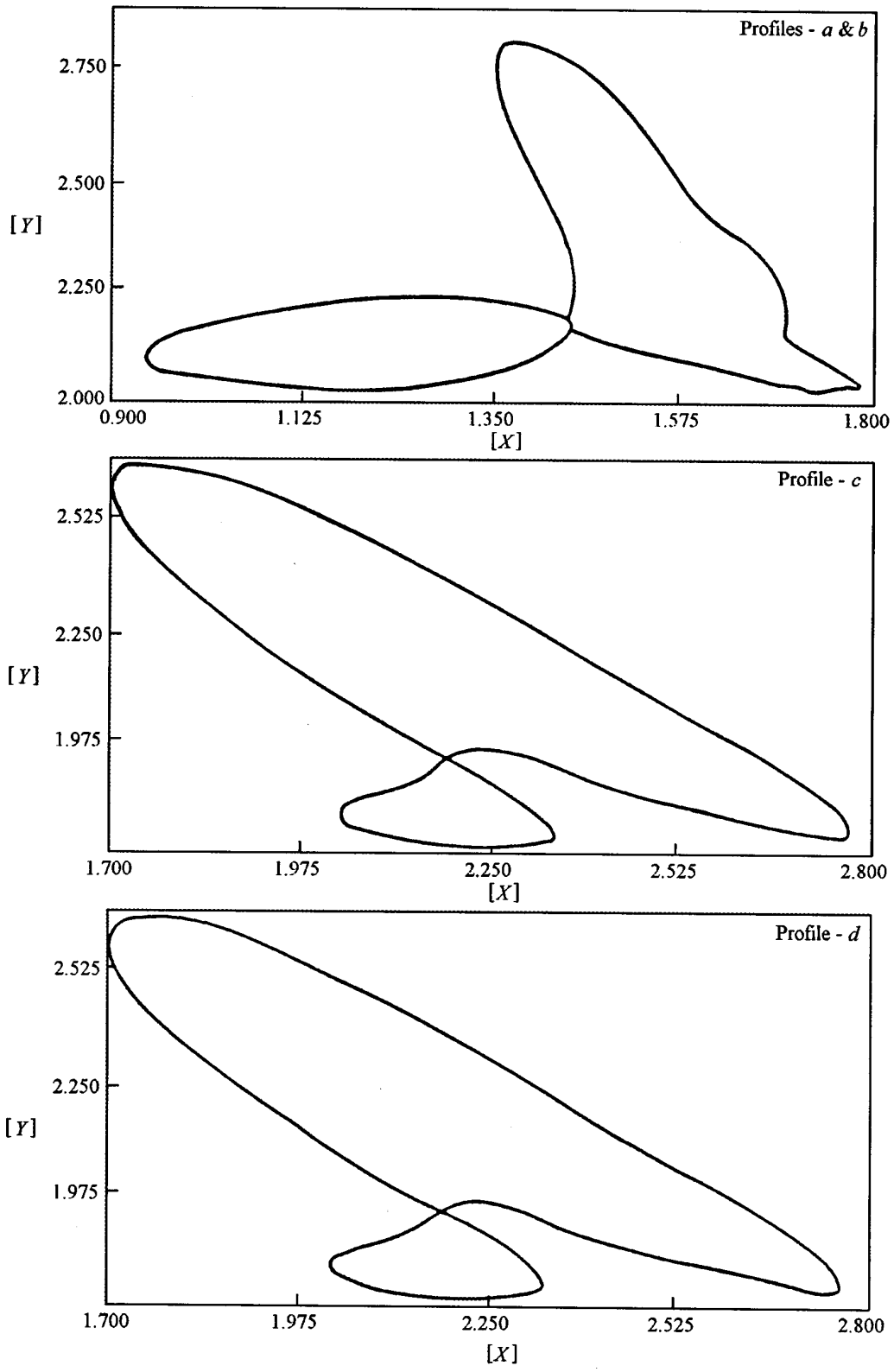


FIG. 11. Phase plane plots of the concentration variables $X$ and $Y$ for the profiles $a$, $b$, $c$, and $d$ with $\tau=2$ and $\sigma=0.02$ for $L=0.1$, $D_x=0.0006$, and $z=0.5$.

facilitate the comparison of the results obtained in the analyses. The deterministic analysis reveals that this unstable state stabilizes at the steady-state solution $a$. With an increase in $\sigma$ from 0.02 to 0.05, for a constant $\tau=2$, the effect is the same as that on solution $a$, as shown earlier in Fig. 3. The temporal evolution of concentration variable $X$ exhibits periodic oscillations after a time ($t=10$) and becomes sustained for low values of $\sigma$ (say 0.02). For higher values of $\sigma$ (0.03–0.05) the oscillations become aperiodic and the solution reaches the trivial solution (curve $e$ in Fig. 2). The effect

of $\tau$, for a constant value of $\sigma = 0.02$, on both the spatial and temporal evolutions is shown in Fig. 6. With increase in $\tau$ from 3 to 20, a stable solution emerges, which is a completely new solution. The temporal structures for this effect reveals that the qualitative features are analogous to that of the effect of $\sigma$, as shown in Fig. 5. The central phase plane plot to this effect, for $\tau = 2$ and $\sigma = 0.02$, is similar to that of the central phase plane plot of profile *a*.

The deterministic and stochastic features of solutions *c* and *d* are shown in Figs. 7–10. These figures clearly reveal the qualitative features of both spatial and temporal evolutions. It is seen from these plots that the effects of $\tau$ and $\sigma$ are to bring about stable transients and periodic oscillations with varying amplitude. The central phase plane plot is depicted in Fig. 11. The trivial solution, i.e., branch 3 (see Fig. 1), is asymptotically stable. Further stochastic analyses of points *p* and *q* on branches 1, 3, and 5 of the bifurcation diagram (Fig. 1) reveal similar effects of $\tau$ and $\sigma$ in bringing about new stable transients.

## CONCLUSION

The effect of external noise in the case of the Brusselator model is to bring about noise-induced transitions, i.e., the system attains a stable steady state not described by the deterministic analysis due to the fluctuations. It has been noted that the increase in the value of $\sigma$ has the effect of bringing the final stabilized state closer to the trivial solution.

The noise-induced transitions are also caused due to the changes in correlation time ($\tau$). However, the new solutions attained by the system do not correspond to any of the deterministic solutions.


[1] M. Sheintuch and R. A. Schmidt, Catal. Rev. Sci. Eng. **15**, 107 (1977).

[2] H. Beusch, P. Fieguth, and E. Wicke, Adv. Chem. Ser. **109**, 615 (1972).

[3] K. F. Jensen and W. H. Ray, Chem. Eng. Sci. **35**, 241 (1980).

[4] R. A. Schmitz, T. Renolag, and A. P. Zioudas, *Dynamics of Modeling of Reactive Systems* (Academic, New York, 1980), p. 177.

[5] S. D. Prasad and B. D. Kulkarni, Chem. Eng. Sci. **37**, 1117 (1982).

[6] P. J. Nandapurkar, V. Hlavacek, and P. Van Rompay, Chem. Eng. Sci. **39**, 1511 (1984).

[7] G. Nicolis and I. Prigogine, *Self Organization in Nonequilibrium Systems* (Wiley, New York, 1977).

[8] I. Prigogine and R. Lefever, J. Chem. Phys. **46**, 3542 (1967).

[9] P. Herschkowitz-Kaufman, Bull. Math. Biol. **37**, 589 (1975).

[10] M. Kubicek and M. Marek, Z. Naturforsch. **35A**, 556 (1980).

[11] V. Hlavacek, R. Jansen, and P. Van Rompay, Z. Naturforsch. **37A**, 39 (1982).

[12] P. J. Nandapurkar, V. Hlavacek, and P. Van Rompay, Chem. Eng. Sci. **41**, 2747 (1986).

[13] N. G. Van Kampen, *Stochastic Processes in Physics, Chemistry, and Natural Sciences* (North-Holland, Amsterdam, 1981).

[14] S. S. Tambe, B. D. Kulkarni, and L. K. Doraiswamy, Chem. Eng. Sci. **40**, 1943 (1985).

[15] W. Horsthemke and R. Lefever, Z. Phys. B **40**, 241 (1980).

[16] J. M. Sancho, M. San Miquel, S. L. Katz, and J. D. Gardiner, Phys. Rev. A **26**, 1589 (1982).

[17] C. W. Gardiner, *Handbook of Stochastic Methods* (Springer-Verlag, Berlin, 1983).

[18] V. Hlavacek and M. Kubicek, *Numerical Solution of Nonlinear Boundary Value Problems with Applications* (Prentice-Hall, New York, 1983).

[19] M. Kubicek and M. Marek, *Computational Methods in Bifurcation Theory and Dissipative Structures* (Springer-Verlag, Berlin, 1983).

[20] Alkis Constantinides, *Applied Numerical Methods with Personal Computers* (McGraw-Hill, New York, 1987).